Early Macular Retinal Ganglion Cell Loss in Dominant Optic Atrophy: Genotype-Phenotype Correlation

PIERO BARBONI, GIACOMO SAVINI, MARIA LUCIA CASCAVILLA, LEONARDO CAPORALI, JACOPO MILESI, ENRICO BORRELLI, CHIARA LA MORGIA, MARIA LUCIA VALENTINO, GIACINTO TRIOLO, ANDREA LEMBO, ARTURO CARTA, ANNAMARIA DE NEGRI, FEDERICO SADUN, GIOVANNI RIZZO, VINCENZO PARISI, LUISA PIERRO, STEFANIA BIANCHI MARZOLI, MASSIMO ZEVIANI, ALFREDO A. SADUN, FRANCESCO BANDELLO, AND VALERIO CARELLI

• PURPOSE: To assess the peripapillary retinal nerve fiber and macular retinal ganglion cell (RGC) loss in patients with dominant optic atrophy (DOA) stratified by OPA1 mutation type.

• DESIGN: Cross-sectional study.

• METHODS: We studied 39 patients from 28 pedigrees with DOA harboring heterozygous mutations in the OPA1 gene along with 45 age-matched healthy subjects. The retinal nerve fiber layer (RNFL) and ganglion cell-inner plexiform layer (GC-IPL) of patients with DOA were evaluated by optical coherence tomography (OCT) and compared to those of controls. Patients' eyes were divided into 4 groups based on increasing severity of visual loss (DOA1 to DOA4) and were stratified by OPA1 mutation type.

• RESULTS: The average thicknesses of the RNFL and GC-IPL were smaller in patients with DOA than in healthy controls ($P < 0.0001$). RNFL analysis showed a significant reduction of the average, superior and inferior quadrants thicknesses in the DOA4 group compared to the DOA1 group ($P = 0.001$, $P = 0.002$ and $P = 0.001$, respectively). GC-IPL analysis showed a significant thinning in the superotemporal and superior sectors in the patients with DOA2 compared to those with DOA1 ($P = 0.046$ and $P = 0.04$, respectively). Stratifying by mutation type, average, superior and nasal RNFL thinning was significantly more severe in missense mutations and had a presumed dominant-negative effect compared to mutations causing haploinsufficiency.

• CONCLUSIONS: The present study demonstrates that in DOA, loss of macular RGCs is the earliest pathologic event, better reflected by GC-IPL measurements, whereas RNFL thickness is a measure of spared axons in late stages of the disease. Thus, mild cases (DOA2) show significant macular RGC loss as opposed to substantial maintenance of RNFL thickness, which is significantly decreased only in severe cases (DOA4). A clear genotype/phenotype correlation emerged, stratifying OCT measures by OPA1 mutation type, missense mutations being the most severe. (Am J Ophthalmol 2014;158:628–636.

DOMINANT OPTIC ATROPHY (DOA) IS A GENETically determined neurodegenerative disorder of retinal ganglion cells (RGCs) that is characterized by slowly progressive bilateral visual loss starting in childhood and ultimately leading to severe optic atrophy.[1,2] However, the disease has incomplete penetrance and variable expression between and within families; it ranges from subclinical manifestations to legal blindness.[1–4]

Most cases of DOA have been associated with mutations in the OPA1 gene on the long arm of chromosome 3q28–q29, which encodes a dynamin-related GTPase targeted to mitochondria.[5] More than 200 OPA1 mutations have been reported (http://mitodyn.org; last update August 20, 2013). Two major mutation categories exist in patients with DOA. Stop-codon, frame-shift and deletion-insertion mutations can be seen throughout the entire gene; these all lead to incomplete transcription and decreased protein content, with haploinsufficiency as the pathogenic mechanism.[5] Missense mutations are thought to act through a dominant negative mechanism, and those affecting the GTPase domain are associated with a syndromic, severe phenotype, defined as DOA "plus."[5] The OPA1 protein localizes to the mitochondrial inner membrane, facing the intermembrane space, and is involved in multiple functions. OPA1 plays a major role

AJO.com Supplemental material available at AJO.com.

Accepted for publication May 27, 2014.

From the Scientific Institute San Raffaele, Milan, Italy (P.B., M.L.C., J.M., E.B., G.T., L.P., F.B.); the Studio Oculistico d'Azeglio, Bologna, Italy (P.B.); the Giovanni Battista Bietti Foundation, Rome, Italy (G.S., V.P.); the Istituto di Ricerca e Cura a Carattere Scientifico (IRCCS), Istituto delle Scienze Neurologiche di Bologna, Bologna, Italy (L.C., C.L.M., M.L.V., G.R.,V.C.); the Department of Biomedical and Neuromotor Sciences (DIBINEM), University of Bologna, Bologna, Italy (C.L.M., M.L.V., G.R., V.C.); the San Giuseppe Hospital, University Eye Clinic, Milan, Italy (A.L.); the Department of Ophthalmology, University of Parma, Italy (A.C.); the Azienda San Camillo-Forlanini, Rome, Italy (A.D.N.); the Ospedale San Giovanni Evangelista, Tivoli, Italy (F.S.); the Neuro-ophthalmology Unit Department of Ophthalmology, Istituto di Ricerca e Cura a Carattere Scientifico (IRCCS) Istituto Auxologico Italiano, Milano, Italy (S.B.M.); the Unit of Molecular Neurogenetics, Foundation C. Besta Neurological Institute, Istituto di Ricerca e Cura a Carattere Scientifico (IRCCS), Milan, Italy (M.Z.); the Medical Research Council Mitochondrial Biology Unit, Cambridge, UK (M.Z); and the Department of Ophthalmology, Keck School of Medicine, University of Southern California, Los Angeles, CA, USA (A.A.S.).

Inquiries to Piero Barboni, Studio Oculistico d'Azeglio, Via d'Azeglio, 5 40123 Bologna, Italy; e-mail: p.barboni@studiodazeglio.it

0002-9394/$36.00
http://dx.doi.org/10.1016/j.ajo.2014.05.034

in regulating mitochondrial network dynamics. In particular, OPA1 induces fusion of the mitochondrial inner membrane, thus impinging on cristae morphology and, by closing cristae junctions, sequestering cytochrome c and modulating apoptosis. OPA1 is also involved in oxidative phosphorylation and the maintenance of mitochondrial DNA.[5] DOA is characterized by loss of visual acuity, cecocentral scotomas, impairment of color vision, and temporal or diffuse atrophy of the optic disc. The incomplete penetrance and the variability of clinical expression may correlate with the extent of optic atrophy.[3,4]

Optical coherence tomography (OCT) is a noninvasive technology that has been successfully used to diagnose and monitor various optic neuropathies, such as glaucoma, Leber hereditary optic neuropathy and nonarteritic ischemic optic neuropathy.[6–9] Time-domain OCT has also been used to study patients with DOA. According to these studies, eyes with DOA show a significant reduction of the retinal nerve fiber layer (RNFL) thickness in all quadrants, with preferential involvement of the temporal and inferior quadrants; the age-related progression of fiber-layer thinning parallels that seen in healthy controls.[10,11] Leber hereditary optic neuropathy is caused by mitochondrial DNA mutations affecting complex I and, as in DOA, is characterized by the early and preferential involvement of the small fibers in the papillomacular bundle, a hallmark of mitochondrial optic neuropathies.[12,13] Furthermore, ONH analysis in DOA has revealed smaller optic discs when compared to healthy controls, suggesting a role of the OPA1 gene in controlling the ONH morphology and, possibly, the complement of retinal nerve fibers at birth.[14]

Spectral-domain OCT has several advantages over time-domain OCT, such as increased repeatability and reproducibility and the possibility of imaging and quantifying macular RCGs by measuring the thickness of the ganglion cell-inner plexiform layer (GC-IPL).[15,16] In the present study, we used spectral-domain OCT to assess (1) the relationship between the RNFL and the GC-IPL thickness in patients with DOA stratified by increasing disease severity based on residual visual acuity; and (2) the genotype-phenotype correlation by comparing OPA1 missense mutations with OPA1 mutations causing haploinsuffiency.

METHODS

• PATIENTS: All patients included in the present study had molecularly confirmed diagnoses of DOA demonstrating an OPA1 mutation, and they were consecutively enrolled and evaluated at the Department of Neurological Sciences at the University of Bologna between 2008 and 2012. We recruited 39 consecutive patients (mean age: 35.6 ± 16.8 years; range, 12–79 years) from 28 unrelated pedigrees. All subjects had extensive ophthalmologic examinations, including best-corrected visual acuity measurement, slit-lamp biomicroscopy, intraocular pressure measurement, indirect ophthalmoscopy, and ONH photography. Exclusion criteria were the presence of any retinal pathology or optic nerve disease other than DOA, and spherical or cylindrical refractive errors higher than 3 and 2 diopters, respectively. All participants gave their informed consent according to the Declaration of Helsinki, and the study was approved by the internal review board at the Department of Neurological Sciences, University of Bologna.

The control group was extracted from a larger sample of 188 healthy subjects who were seen during routine ophthalmologic examinations. Inclusion criteria were the following: best-corrected visual acuity of at least 0.8 (decimal fraction); refractive error between −3 and +3 diopters of sphere and between −2 and +2 diopters of cylinder; normal (<21 mm Hg) intraocular pressure; normal appearance of the optic disc; normal visual field (the latter was examined with a Swedish interactive thresholding algorithm, SITA 24-2, standard test in all subjects by using the Humphrey VF analyzer, HFA II 750-4.1 2005; Carl Zeiss Meditec, Dublin, California, USA); no significant ocular disease found by routine ophthalmologic examination; and no family history of glaucoma or systemic diseases with possible ocular involvement such as diabetes mellitus. From this sample, we randomly selected 45 eyes of 45 subjects matching the patients' groups for age, age being shown to influence peripapillary RNFL thickness, as measured by time-domain OCT and spectral-domain OCT.[17–22] Age also has been shown to influence the GC-IPL thickness.[16]

• INSTRUMENTATION AND PROCEDURES: All subjects underwent measurements of RNFL thickness and GC-IPL thickness by spectral-domain OCT (Cirrus SD-OCT, software v 6.0; Carl Zeiss Meditec). All scans were acquired by the same operator using the Optic Disc Cube 200 × 200 and the Macular Cube 512 × 128 protocols in eyes without pupil dilation. After each patient had been properly seated and aligned, the iris was brought into view using the mouse-driven alignment system, and the ophthalmoscopic image was focused. To acquire the Optic Disc Cube, the ONH was centered on the live image, and centering and enhancement were optimized. After the scanning process was launched, the instrument's 840 nm wavelength laser beam generated a cube of data measuring 6 mm × 6 mm after scanning a series of 200 B-scans with 200 A-scans per B-scan (40,000 points) in 1.5 seconds (27,000 A-scans/sec). Cirrus spectral-domain OCT algorithms were used to find the optic disc and automatically place a calculation circle 3.46 mm in diameter symmetrically around it. Layer-seeking algorithms were used to find the RNFL inner (anterior) boundary and the RNFL outer (posterior) boundary for the entire cube except the optic disc. The system extracted from the data cube 256 A-scan samples along the path of the calculation circle. The resulting temporal, superior, nasal, inferior profile map is equivalent to the Stratus peripapillary RNFL scan.

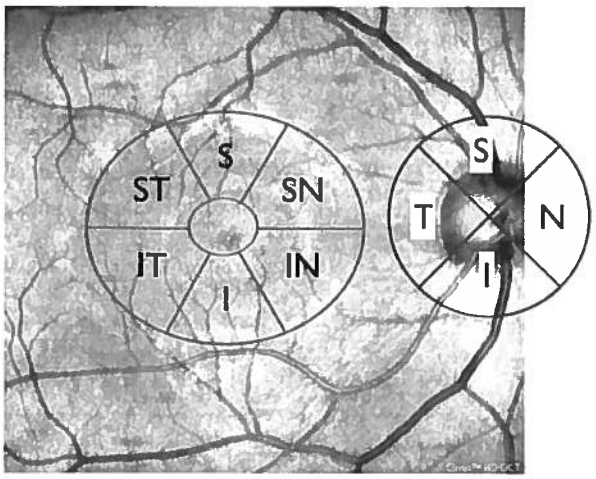

FIGURE 1. The thicknesses of the 4 retinal nerve fiber layer quadrants (temporal, superior, nasal, inferior) and the 6 ganglion cell-inner plexiform layer sectors (superotemporal, superior, superonasal, inferonasal, inferior, inferotemporal) were measured from circular scans around the disc and from the elliptical annulus centered on the fovea, respectively.

The ONH parameters reported resulted from a fully automatic algorithm that defines both the optic disc and the cup margins within the 3-dimensional data cube. The disc margin was defined as the termination of the Bruch membrane (also referred to as the neural canal opening or Bruch's membrane opening).[23]

To acquire the Macular Cube, the patient was asked to fixate on the central target. The ganglion cell analysis algorithm detected and measured the thickness of the macular GC-IPL within a 14.13-mm^2 elliptical annulus area centered on the fovea (Figure 1). The size and shape of the annulus were chosen for conformance to the real anatomy, and this annulus corresponded to the area where the RGC layer is thickest in normal eyes. The ganglion cell analysis algorithm processed data from 3-dimensional volume scans and measured the thickness of the macular GC-IPL. The average, minimum, and 6 sectoral (superotemporal, superior, superonasal, inferonasal, inferior, and inferotemporal) GC-IPL thicknesses were measured from the elliptical annulus centered on the fovea (Figure 1). A detailed description of how this algorithm operates has been published in detail.[16]

Only high-quality scans, defined as scans with signal strength ≥6, without RNFL discontinuity or misalignment, involuntary saccade, or blinking artifacts and absence of algorithm segmentation failure on careful visual inspection were used for analysis.

• STATISTICS: The patients' eyes were divided into different groups based on visual acuity: group 1 (DOA1) between 1.0 and 0.6; group 2 (DOA2) between 0.5 and 0.4; group 3 (DOA3) between 0.32 and 0.25; and group 4 (DOA4) less than 0.25 of visual acuity. These groups were established using increments of visual acuity of 0.25. The patients with visual acuity better than 0.25 were further stratified into 3 subgroups representing different degrees of visual function. In the control group, only 1 eye, randomly chosen, was considered for statistical evaluation in each subject. Moreover, the data from patients with DOA were also stratified by OPA1 mutation category: mutations causing haploinsufficiency (DOA-H) or missense mutations (DOA-M). The groups were compared by 1-way analysis of variance (ANOVA) with Bonferroni post hoc tests. Linear regressions were used to search for correlations between visual acuity and RNFL and GC-IPL measurements, introducing age and sex as covariates. All statistical analyses were performed using SPSS (IBM v 20; PASW, Chicago, Illinois, USA) and a P value <0.05 was considered statistically significant after appropriate correction for multiple comparisons.

RESULTS

FOR THIS STUDY, WE COLLECTED 39 DOA PATIENTS FROM 28 DOA pedigrees that harbored a pathogenic heterozygous mutation in the OPA1 gene (Table 1). The control group consisted of 45 age-matched subjects. All patients met the inclusion criteria.

Table 1 shows the OPA1 mutation types in the 28 pedigrees stratified by mutational category (mutations causing haploinsufficiency vs missense mutations). Patients from pedigrees carrying the same mutation were pooled. Most mutations were well-established OPA1 pathogenic mutations listed in the OPA1 mutation database (mitodyn.org); some mutations have been reported recently[11,14] or are unpublished.

• OPTICAL COHERENCE TOMOGRAPHY MEASUREMENTS IN DOMINANT OPTIC ATROPHY GROUPED BY CATEGORIES OF INCREASING VISUAL ACUITY LOSS SEVERITY: *Optic nerve head.* Comparison of the optic disc area by 1-way ANOVA disclosed significant differences (P = 0.032) in the 5 groups. Only the DOA group with the lowest visual acuity (DOA4) showed a significantly smaller disc area compared to the control group (P = 0.024). Post hoc testing failed to disclose differences among the other 4 DOA groups (DOA1-DOA3) and the control group (Table 2).

Retinal nerve fiber layer. One-way ANOVA revealed a significant difference ($P < 0.0001$) in the peripapillary RNFL thickness for the 360 degree average value as well as in each quadrant. The post hoc test detected a significant reduction in each quadrant in all DOA groups compared to controls ($P < 0.0001$). Moreover, a significant reduction was observed in the average, superior and inferior RNFL quadrant thicknesses in groups with

TABLE 1. OPA1 Mutations in Patients with Dominant Optic Atrophy, Described According to Variant 1, RefSeq: NM_015560.2

No. Pedigree	No. Affected Patients	*OPA1* Mutations		*OPA1* Exon	M/H	Note
5	9	*c.2708-2711delTTAG*	*p.V903fs*	*27*	H	
2	3	*c.2825-2828delAGTT*	*p.V942fs*	*28*	H	
1	1	*c.113-130del18*	*p.38-43del6*	*2*	H	
1	1	*c.1669C>T*	*p.R557X*	*17*	H	
1	1	*c.1724-1725delAA*	*p.R557X*	*18*	H	*
1	1	*c.1770G>A*	*spice defect*	*18*	H	*
1	1	*c.1783insT*	*p.F594fs*	*19*	H	*
1	2	*c.2193-2196dupAGAC*	*p.D732fs*	*22*	H	*
1	1	*c.2671-2694dup24*	*p.891-898dup8*	*26*	H	*
1	1	*c.2708-2A>T*	*splice defect*	*27*	H	11
1	2	*c.2819-2A>C*	*splice defect*	*28*	H	14
1	1	*c.703C>T*	*p.R235X*	*7*	H	
1	1	*c.870+5G>A*	*splice defect*	*8*	H	
1	2	*c.889C>T*	*p.Q297X*	*9*	H	
1	1	*c.1770+1 delG*	*splice defect*	*17*	H	
1	1	*c.1516+1G>C*	*splice defect*	*15*	H	
1	2	*c.2815delC*	*p.L939fs*	*27*	H	11
2	4	*c.1409A>G*	*p.D470G*	*14*	M	
1	1	*c.1778 T>C*	*p.L593P*	*19*	M	
1	1	*c.869 G>A*	*p.R290Q*	*8*	M	
1	1	*c.2729T>A*	*p.V910D*	*27*	M	11
1	1	*c.1807G>C*	*p.D603H*	*19*	M	*

H = mutation causing haploinsuffiency; M = missense mutation; * = unpublished mutation but with clear pathogenicity.

DOA1, ($P = 0.001$, $P = 0.002$ and $P = 0.001$, respectively); DOA2 ($P = 0.004$, $P = 0.003$ and $P = 0.023$, respectively); and DOA3 ($P = 0.013$, $P = 0.016$ and $P = 0.025$, respectively) compared to the DOA4 group, which exhibited the lowest values.

The average percentage of reduction of the RNFL thicknesses in the 4 DOA groups compared to controls was more evident in the temporal and inferior quadrants (mean ratio −56% and −47%, respectively) and was less pronounced in the superior and nasal quadrants (mean ratio −35% and −29%, respectively) (Table 3) (Figure 2). Moreover, considering all 4 quadrants, the reduction of the RNFL thickness was more evident between DOA3 and DOA4 (mean ratio −10%) than between DOA1 and DOA3 (mean ratio −4%).

Ganglion cell-inner plexiform layer analysis. The GC-IPL thickness was significantly lower in all macular sectors, on the average and in the minimum value, compared to the control group (ANOVA, $P < 0.0001$). The post hoc test also demonstrated significant thinning of all sectors in all groups with DOA compared to the controls ($P < 0.0001$). The comparison among the 4 groups with DOA showed significant reductions in the superotemporal and superior sectors between the DOA1 and DOA2 groups ($P = 0.046$ and $P = 0.04$, respectively); on average, reductions in the superotemporal and superior and superonasal sectors in DOA1 and DOA3 ($P = 0.025$, $P = 0.001$, $P < 0.0001$, and $P = 0.049$, respectively); on average, minimum reductions in the inferotemporal, superotemporal, superior, and superonasal sectors in the DOA1 and DOA4 groups ($P < 0.0001$, $P = 0.04$, $P < 0.0001$, $P < 0.0001$, $P < 0.0001$, and $P = 0.038$, respectively); and reductions in the in inferotemporal and superotemporal sectors in DOA2 and DOA4 ($P = 0.01$ and $P < 0.005$, respectively). The remaining sectors of the 4 DOA groups revealed similar loss of ganglion cells, independent of the residual visual acuity.

The percentage of reduction of the GC-IPL thickness in the DOA1 group was more evident in the superonasal, inferonasal and inferior sectors (mean ratios −38%, −38% and −36%, respectively) and less pronounced in the inferotemporal, superotemporal and superior sectors (mean ratios −33%, −27% and −29%, respectively) compared to controls. In the other DOA groups (DOA2-DOA4), the mean ratios increased in a similar fashion (Table 3) (Figure 2). Moreover, considering all sectors, the reduction of the GC-IPL thickness was more evident between DOA1 and DOA3 (mean ratio −8%) than between DOA3 and DOA4 (mean ratio −1%).

Optical coherence tomography measurements in dominant optic atrophy grouped by different OPA1 mutations. After stratifying DOA patients by OPA1 mutation (Table 4),

TABLE 2. Best-Corrected Visual Acuity, Age, Optic Disc Area, Retinal Nerve Fiber Layer, and Macular Ganglion Cell-Inner Plexiform Layer Thickness in Patients with Dominant Optic Atrophy and in the Control Group

	Controls (Mean ± SD) n = 45	DOA1 (Mean ± SD) n = 11	DOA2 (Mean ± SD) n = 16	DOA3 (Mean ± SD) n = 13	DOA4 (Mean ± SD) n = 38
BCVA	1.0 ± 0.0	0.70 ± 0.45	0.46 ± 0.50	0.29 ± 0.03	0.11 ± 0.06
Age	39.0 ± 16.9	44.2 ± 13.8	28.2 ± 13.6	30.0 ± 11.8	39.1 ± 19.6
Optic disc area (mm^2)	1.9 ±0.3	1.8 ± 0.3	1.9 ± 0.4	1.8 ± 0.4	1.6 ± 0.4
RNFL thickness (μm)					
Avg	96.1 ± 9.9	61.4 ± 10.4**	57.6 ± 9.3*	57.4 ± 7.6*	46.7 ± 11.0
Temp	66.4 ± 10.5	31.8 ± 7.1	28.4 ± 6.1	29.7 ± 7.6	25.6 ± 9.0
Sup	119.5 ± 14.9	83.7 ± 15.9*	80.8 ± 14.9*	79.6 ± 14.3*	64.6 ± 13.2
Nas	71.8 ± 11.5	53.8 ± 11.2	53.9 ± 11.0	51.6 ± 10.6	44.5 ± 12.7
Inf	126.5 ± 18.3	75.9 ± 13.4**	68.0 ± 13.7*	69.0 ± 11.2*	53.4 ± 14.9
GC-IPL thickness (μm)					
Avg	83.3 ± 4.8	55.4 ± 6.3**	51.7 ± 4.0	49.6 ± 2.4†	58.6 ± 4.3
Min	82.1 ± 5.2	49.3 ± 5.5*	46.6 ± 4.4	44.8 ± 2.8	42.9 ± 5.4
IT	84.2 ± 5.4	56.4 ± 6.3**	53.1 ± 4.0*	51.2 ± 3.2	48.2 ± 4.6
ST	82.1 ± 5.0	59.7 ± 8.1**	53.8 ± 4.2†,*	51.2 ± 2.8††	48.2 ± 5.4
S	83.7 ± 5.0	59.5 ± 10.2**	51.9 ± 4.5†	50.3 ± 2.7††	49.9 ± 4.7
SN	84.7 ± 5.4	52.7 ± 6.7*	50.0 ± 4.7	46.8 ± 3.4†	47.6 ± 4.5
IN	83.4 ± 5.2	51.5 ± 4.5	49.4 ± 4.5	47.8 ± 2.5	47.3 ± 4.6
I	82.3 ± 5.3	52.9 ± 4.9	50.8 ± 4.4	49.1 ± 3.5	49.2 ± 4.2

Avg = average; BCVA = best-corrected visual acuity; DOA = dominant optic atrophy; GC-IPL = macular ganglion cell-inner plexiform layer; I = inferior sector; IN = inferonasal sector; Inf = inferior quadrant; IT = inferotemporal sector; SD = standard deviation; Min = minimum; n = number of eyes; Nas = nasal quadrant; RNFL = retinal nerve fiber layer; S = superior sector; SN = superonasal sector; ST = superotemporal sector; Sup = superior quadrant; Temp = temporal quadrant.

*$P < 0.05$ Bonferroni post hoc test.

**$P < 0.001$ Bonferroni post hoc test compared to DOA 4.

†$P < 0.05$ Bonferroni post hoc test.

††$P < 0.001$ Bonferroni post hoc test compared to DOA 1.

TABLE 3. Percentage of Reduction Compared to Controls in the 4 Dominant Optic Atrophy Subgroups

DOA Groups	RNFL Avg	Temp	Sup	Nas	Inf	GC-IPL Avg	GC-IPL Min	IT	ST	S	SN	IN	I
DOA1	−36	−52	−30	−25	−40	−34	−40	−33	−27	−29	−38	−38	−36
DOA2	−40	−57	−32	−25	−46	−38	−43	−37	−34	−38	−41	−41	−38
DOA3	−40	−55	−33	−28	−45	−40	−45	−39	−38	−40	−45	−43	−40
DOA4	−51	−61	−46	−38	−58	−42	−48	−43	−41	−40	−44	−43	−40
DOA1 vs DOA3	−4	−3	−3	−3	−5	−7	−4	−6	−10	−11	−7	−5	−5
DOA3 vs DOA4	−11	−6	−13	−10	−12	−1	−10	−4	−4	−0	−1	−1	−0

Avg = average; DOA = dominant optic atrophy; GC-IPL = macular ganglion cell-inner plexiform layer; I = inferior sector; IN = inferonasal sector; Inf = inferior quadrant; IT = inferotemporal sector; Min = minimum; Nas = nasal quadrant; RNFL = retinal nerve fiber layer; ST = superotemporal sector; Sup = superior quadrant; S = superior sector; SN = superonasal sector; Temp = temporal quadrant.

1-way ANOVA revealed a significant difference in the visual acuity but not in the age or in the optic disc area.

Retinal nerve fiber layer and ganglion cell-inner plexiform layer analysis. The post hoc test detected a significant reduction in DOA-M compared to DOA-H in the average, superior and nasal RNFL and in the inferotemporal GC-IPL sector measurements.

Linear regression between the entire optical coherence tomography data set and visual acuity. Linear regression using the whole OCT dataset, with age and sex as covariates, showed that RNFL thinning correlated with visual acuity only in average, superior and inferior quadrant measurements, whereas GC-IPL thinning significantly correlated with visual acuity loss (Table 5) (Supplemental Figure 1, Supplemental Figure 2).

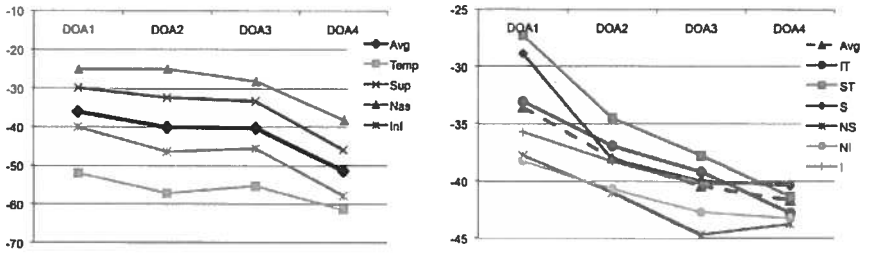

FIGURE 2. The first graph (left) represents the pattern of retinal nerve fiber layer thinning in the average and the 4 quadrants in the 4 dominant optic atrophy groups. It shows the steepest decline between DOA3 and DOA4 groups. The second graph (right) shows the pattern of ganglion cell-inner plexiform layer thinning in the average and the 6 sectors in the 4 DOA groups. It shows the steep decrease between the DOA1 and DOA2 groups and less of a gradient in the other groups, DOA2 to DOA4.

DISCUSSION

THIS STUDY, CARRIED OUT BY SPECTRAL-DOMAIN OCT, combined the assessments of both RNFL and GC-IPL thickness in patients with DOA, categorized by increasing severity of visual acuity loss. Our results showed a profound and early RGC loss in the macula, as exemplified by the steep decrease between DOA1 and DOA2 groups and then the less pronounced changes among the other DOA groups despite the increasing severity of visual loss (DOA2 to DOA4) (Figure 2). This pattern is different from that seen with measures of RNFL thickness, which show the steepest decline between the DOA3 and DOA4 groups (Figure 2). Insofar as the paradigm is early involvement of macular RGCs, later, the changes are better reflected by a larger retinal area, which contributes to the RNFL. A second finding of our study is that the residual visual acuity may be dependent on the remaining fibers of the superior and nasal quadrants that showed the most preserved RNFL thicknesses and, correspondingly, the temporal sectors of the GC-IPL (inferotemporal and superotemporal). Symmetrically, superonasal and inferonasal GC-IPL sectors as well as the temporal RNFL quadrant were the thinnest in all groups, corresponding to the papillomacular bundle being most affected. When these results were stratified by OPA1 mutation type, we found that missense mutations had the most severe reductions in both RNFL and GC-IPL thickness. We also used the entire data set of OCT measurements to run a linear regression with age and sex as covariates, thus avoiding the categoric grouping by severity of visual acuity. We found that GC-IPL thinning was significantly correlated with visual acuity loss, whereas this correlation was less stringent for RNFL thinning.

The only 2 histologic studies of post mortem ocular tissues from patients with DOA available to date showed RGC loss in the retina, reflected as loss of axons (with gliotic and myelin changes) in the optic nerve.[24,25] Since the availability of OCT, it has been well established that, in DOA, peripapillary RNFL loss occurs in consequence to axonal degeneration.[10,11,26] Insofar as average RNFL reflects global RGC loss and the area of the retina contributing goes, as the distance from the fovea is squared, there will be some weighting for the mid or far periphery. This may be somewhat different from Leber hereditary optic neuropathy, where the central scotoma is often much larger than in DOA. More recently, it has been reported, by studies of an OPA1-mutant mouse model of DOA, that the first morphologic evidence of disease is a RGC dendropathy.[27,28] In fact, the earliest pathologic changes observed in the retinas of these animals were dendritic pruning and marked reduction in synaptic connectivity, qualifying a dendropathy in the absence of any other appreciable pathology of RGC somata and axons. This might be understood in light of the crucial role played by OPA1 and mitochondrial fusion in maintaining dendrites and their synapses.[29,30] Unfortunately, the mouse has no fovea, so it would be interesting to see, in another animal model, whether these dendritic changes first occur in RGCs that are located near the fovea. Our present human study, being cross-sectional in design, cannot definitely establish the pattern of RGC loss in the natural history of the pathologic process.

We confirmed previous results showing that patients with DOA demonstrate significant reductions in average RNFL thickness. In particular, the present study of the RNFL quadrants detected a greater thinning of the temperal inferior fibers, followed by the superior and nasal fibers. These data are consistent with previous time-domain OCT studies that show the selectivity of the pathologic process in DOA, as in other mitochondrial optic neuropathies, for the papillomacular bundle.[10,11] This probably reflects a predilection for the smallest fibers, most of which constitute the papillomacular bundle. A mathematical model that takes into account issues of surface area to volume accurately predicts the order of fiber involvement in mitochondrial diseases.[12,13]

The current study exploits technological advancements in spectral-domain OCT, including repeatibility[31] and

TABLE 4. Best Corrected Visual Acuity, Age, Optic Disc Area, Retinal Nerve Fiber Layer and Macular Ganglion Cell-Inner Plexiform Layer Thickness in Patients with Dominant Optic Atrophy and in the Control Group

	Controls (Mean ± SD) n = 45	DOA-M (Mean ± SD) n = 16	DOA-H (Mean ± SD) n = 62
BCVA	1.0 ± 0.0	0.19 ± 0.19	0.32 ± 0.22*
Age	39.0 ± 16.9	38.6 ± 15.9	35.4 ± 17.5
Optic disc area (mm^2)	1.9 ± 0.3	1.7 ± 0.4	1.7 ± 0.4
RNFL thickness (μm)			
Avg	96.1 ± 9.9	45.1 ± 13.1	54.7 ± 10.4*
Temp	66.4 ± 10.5	25.9 ± 8.1	28.2 ± 8.2
Sup	119.5 ± 14.9	62.7 ± 15.2	75.8 ± 15.5*
Nas	71.8 ± 11.5	38.2 ± 9.9	51.7 ± 11.2**
Inf	126.5 ± 18.3	58.4 ± 24.4	63.1 ± 13.6
GC-IPL thickness (μm)			
Avg	83.3 ± 4.8	48.7 ± 5.4	50.8 ± 4.7
Min	82.1 ± 5.2	43.3 ± 5.8	45.3 ± 5.1
IT	84.2 ± 5.4	47.8 ± 6.2	51.7 ± 4.9*
ST	82.1 ± 5.0	48.6 ± 7.1	52.3 ± 6.2
S	83.7 ± 5.0	49.7 ± 5.9	52.3 ± 6.4
SN	84.7 ± 5.4	47.7 ± 5.5	49.0 ± 5.0
IN	83.4 ± 5.2	47.7 ± 5.5	48.6 ± 4.2
I	82.3 ± 5.3	48.7 ± 4.4	50.4 ± 4.3

Avg = average; BCVA = best-corrected visual acuity; DOA-H = DOA with mutation causing haploinsuffiency; DOA-M = DOA with missense mutation; GC-IPL = macular ganglion cell-inner plexiform layer; I = inferior sector; IN = inferonasal sector; Inf = inferior quadrant; IT = inferotemporal sector; Min = minimum; n = number of eyes; Nas = nasal quadrant; RNFL = retinal nerve fiber layer; S = superior sector; SD = standard deviation; SN = superonasal sector; ST = superotemporal sector; Sup = superior quadrant; Temp = temporal quadrant.

*$P < 0.05$ Bonferroni post hoc test.

**$P < 0.001$ between DOA-M and DOA-H.

TABLE 5. Linear Regression Between Macular Ganglion Cell-Inner Plexiform Layer Thickness, Retinal Nerve Fiber Layer Thickness and Best-Corrected Visual Acuity in Patients with Dominant Optic Atrophy

GC-IPL Thickness (μm) (n 78; Mean ± SD)		BCVA R	BCVA P*
Avg	50.4 ± 4.9	0.61	<0.0001
Min	44.9 ± 5.3	0.51	<0.001
IT	50.9 ± 5.4	0.66	<0.0001
ST	51.5 ± 6.6	0.72	<0.0001
S	51.8 ± 6.3	0.63	<0.0001
SN	48.7 ± 5.0	0.50	0.001
IN	48.4 ± 4.5	0.42	<0.05
I	50.0 ± 4.4	0.41	<0.05
RNFL Thickness (μm) (n 78; Mean ± SD)		**BCVA R**	**BCVA P***
Avg	52.8 ± 11.6	0.57	<0.0001
Temp	27.7 ± 8.2	0.34	0.32
Sup	73.1 ± 16.2	0.57	<0.0001
Nas	48.9 ± 12.2	0.40	0.06
Inf	62.2 ± 16.3	0.57	<0.0001

Avg = average; BCVA = best corrected visual acuity; GC-IPL = macular ganglion cell-inner plexiform layer; I = inferior sector; IN = inferonasal sector; Inf = inferior quadrant; IT = inferotemporal sector; Min = minimum; n = number of eyes; Nas = nasal quadrant; RNFL = retinal nerve fiber layer; S = superior sector; SD = standard deviation; SN = superonasal sector; ST = superotemporal sector; Sup = superior quadrant; Temp = temporal quadrant.

Note: Age and sex were used as covariates.

*P values were corrected for multiple tests according to Bonferroni post hoc tests.

the possibility of assessing the macular area and measuring the GC-IPLs. In fact, the combined information derived from the assessment of both provides insights, via macular GC-IPL thickness, into the early stages of the disease and, via the peripapillary RNFL thickness, into the late stages of the disease. A seminal study of macular RGCs by OCT segmentation reported a reduction of the inner retinal thickness, with preservation of the photoreceptor layer.[32] A recent study of patients with DOA and with a single mutation type leading to haploinsufficiency reached similar conclusions.[33] However, the analysis of our study considered both RNFL thickness and GC-IPL thickness in relation to visual acuity and allowed us to appreciate a pattern that probably reflects the natural history of the disease. This pattern has been extrapolated by cross-sectional collected data, and the limitation of this present approach is that a natural history of DOA can be properly characterized only by a long-term longitudinal follow-up study. Notwithstanding, these two OCT indices, correlated with visual acuity and visual field assessments, may become part of an algorithm describing the disease stage. Such OCT measurements will be also significant endpoints to evaluate therapeutic efficacy in upcoming trials with new molecules.[34]

We stratified the spectral-domain OCT measurements by OPA1 mutation type, considering first the wide categories of mutations predicted to lead to a truncated protein and haploinsufficiency (DOA-H),[3,5,35,36] and then those that induce an amino acid change (missense mutations) for which a dominant negative mechanism is postulated (DOA-M),[3,5] and a clear difference emerged.[5] Missense mutations displayed the most severe phenotype. A previous study limited to the assessment of RNFL thickness by time-domain OCT reported that DOA "plus" involved a particularly severe RNFL thinning.[26,37,38] Notably, in our case series, only 1 patient could be classified as DOA "plus",

with the features of optic atrophy and sensorineural deafness. This patient had a missense mutation affecting the GTPase domain, whereas missense mutations are highly associated with the DOA "plus" phenotype.[37,38] However, all the remaining 7 cases with missense mutations had the classical nonsyndromic DOA presentation of isolated optic atrophy. Thus, the different pathogenic mechanisms between missense mutations and mutations causing haploinsufficiency might drive the severity of the optic atrophy. The most severe visual loss in patients carrying OPA1 missense mutations was also shown by a previous study of a large DOA cohort.[3]

In conclusion, the present study demonstrates that the loss of RGCs occurs first in the macula where it is best visualized by GC-IPL measures; later, more global loss of RGCs are best captured by RNFL thickness measurements. Missense mutations in the OPA1 gene predict a more severe prognosis.

THIS STUDY WAS SUPPORTED IN PART BY TELETHON GRANTS GGP06233 (TO V.C.) AND GPP10005 (TO M.Z. AND V.C.). STUDY design and conduct (P.B., G.S., M.L.C., A.A.S., F.B., V.C.); Data collection, management and analysis (P.B., G.S., M.L.C., L.C., J.M., E.B., C.L.M., M.L.V., G.T., A.L., A.C., A.N.D., F.S., G.R., V.P., L.P., S.B.M., M.Z., A.A.S., F.B., V.C.); Interpretation of data (P.B., G.S., M.L.C., A.A.S., F.B., V.C.); Preparation of manuscript (P.B., G.S., M.L.C., A.A.S., F.B., V.C.); and Review or approval of manuscript (P.B., G.S., M.L.C., A.A.S., F.B., V.C.).

REFERENCES

1. Kjer P. Infantile optic atrophy with dominant mode of inheritance: a clinical and genetic study of 19 Danish families. *Acta Ophthalmol Suppl* 1959;164(Supp 54):1–147.
2. Newman NJ. Hereditary optic neuropathies. In: Miller NR, Newman NJ, Biousse V, Kerrison JB, eds. Walsh and Hoyt's Clinical Neuro-Ophthalmology. 6th ed, vol. 1. Philadelphia, PA: Lippincott Williams & Wilkins; 2005: 465–501.
3. Yu-Wai-Man P, Griffiths PG, Burke A, et al. The prevalence and natural history of dominant optic atrophy due to OPA1 mutations. *Ophthalmology* 2010;117(8):1538–1546.
4. Cohn AC, Toomes C, Hewitt AW, et al. The natural history of OPA1-related autosomal dominant optic atrophy. *Br J Ophthalmol* 92(10):1333–1336.
5. Yu-Wai-Man P, Griffiths PG, Chinnery PF. Mitochondrial optic neuropathies-disease mechanisms and therapeutic strategies. *Prog Retin Eye Res* 2011;30(2):81–114.
6. Savini G, Carbonelli M, Barboni P. Spectral-domain optical coherence tomography for the diagnosis and follow-up of glaucoma. *Curr Opin Ophthalmol* 2011;22(2):115–123.
7. Barboni P, Savini G, Valentino ML, et al. Retinal nerve fiber layer evaluation by optical coherence tomography in Leber's hereditary optic neuropathy. *Ophthalmology* 2005;112(1): 120–126.
8. Savini G, Barboni P, Valentino ML, et al. Retinal nerve fiber layer evaluation by optical coherence tomography in unaffected carriers with Leber's hereditary optic neuropathy mutations. *Ophthalmology* 2005;112(1):127–131.
9. Bellusci C, Savini G, Carbonelli M, Carelli V, Sadun AA, Barboni P. Retinal nerve fiber layer thickness in nonarteritic anterior ischemic optic neuropathy: OCT characterization of the acute and resolving phases. *Graefes Arch Clin Exp Ophthalmol* 2008;246(5):641–647.
10. Milea D, Sander B, Wegener M, et al. Axonal loss occurs early in dominant optic atrophy. *Acta Ophthalmol* 2010; 88(3):342–346.
11. Barboni P, Savini G, Parisi V, et al. Retinal nerve fiber layer thickness in dominant optic atrophy measurements by optical coherence tomography and correlation with age. *Ophthalmology* 2011;118(10):2076–2080.
12. Sadun AA, Win PH, Ross-Cisneros FN, Walker SO, Carelli V. Leber's hereditary optic neuropathy differentially affects smaller axons in the optic nerve. *Trans Am Ophthalmol Soc* 2000;98:223–232; discussion 232–235.
13. Pan BX, Ross-Cisneros FN, Carelli V, et al. Mathematically modeling the involvement of axons in Leber's hereditary optic neuropathy. *Invest Ophthalmol Vis Sci* 2012;53(12):7608–7617.
14. Barboni P, Carbonelli M, Savini G, et al. OPA1 mutations associated with dominant optic atrophy influence optic nerve head size. *Ophthalmology* 2010;117(8):1547–1553.
15. Leung CK, Cheung CY, Weinreb RN, et al. Retinal nerve fiber layer imaging with spectral domain optical coherence tomography: a variability and diagnostic performance study. *Ophthalmology* 2009;116(7):1257–1263.
16. Mwanza JC, Oakley JD, Budenz DL, Chang RT, Knight OJ, Feuer WJ. Macular ganglion cell-inner plexiform layer: automated detection and thickness reproducibility with spectral domain-optical coherence tomography in glaucoma. *Invest Ophthalmol Vis Sci* 2011;52(11):8323–8329.
17. Parikh RS, Parikh SR, Sekhar GC, Prabakaran S, Babu JG, Thomas R. Normal age-related decay of retinal nerve fiber layer thickness. *Ophthalmology* 2007;114(5):921–926.
18. Sung KR, Wollstein G, Bilonick RA, et al. Effects of age on optical coherence tomography measurements of healthy retinal nerve fiber layer, macula and optic nerve head. *Ophthalmology* 2009;116(6):1119–1124.
19. Budenz DL, Anderson DR, Varma R, et al. Determinants of normal retinal nerve fiber layer thickness measured by Stratus OCT. *Ophthalmology* 2007;114(6):1046–1052.
20. Bendschneider D, Tornow RP, Horn FK, et al. Retinal nerve fiber layer thickness in normals measured by spectral domain OCT. *J Glaucoma* 2010;19(7):475–482.
21. Alasil T, Wang K, Keane PA, et al. Analysis of normal retinal nerve fiber layer thickness by age, sex and race using spectral domain optical coherence tomography. *J Glaucoma* 2013; 22(7):532–541.
22. Knight OJ, Girkin CA, Budenz DL, Durbin MK, Feuer WJ. Effect of race, age, and axial length on optic nerve head parameters and retinal nerve fiber layer thickness measured by Cirrus HD-OCT. *Arch Ophthalmol* 2012;130(3):312–318.
23. Strouthidis NG, Yang H, Reynaud JF, et al. Comparison of clinical and spectral domain optical coherence tomography

optic disc margin anatomy. *Invest Ophthalmol Vis Sci* 2009; 50(10):4709–4718.
24. Johnston PB, Gaster RN, Smith VC, Tripathi RC. Clinicopathologic study of autosomal dominant optic atrophy. *Am J Ophthalmol* 1979;88(5):868–875.
25. Kjer P, Jensen OA, Klinken L. Histopathology of eye, optic-nerve and brain in a case of dominant optic atrophy. *Acta Ophthalmol (Copenh)* 1983;61(2):300–312.
26. Yu-Wai-Man P, Bailie M, Atawan A, Chinnery PF, Griffiths PG. Pattern of retinal ganglion cell loss in dominant optic atrophy due to OPA1 mutations. *Eye (Lond)* 2011; 25(5):596–602.
27. Williams PA, Morgan JE, Votruba M. Opa1 deficiency in a mouse model of dominant optic atrophy leads to retinal ganglion cell dendropathy. *Brain* 2010;133(10):2942–2951.
28. Williams PA, Piechota M, von Ruhland C, Taylor E, Morgan JE, Votruba M. Opa1 is essential for retinal ganglion cell synaptic architecture and connectivity. *Brain* 2012; 135(Pt 2):493–505.
29. Li Z, Okamoto K, Hayashi Y, Sheng M. The importance of dendritic mitochondria in the morphogenesis and plasticity of spines and synapses. *Cell* 2004;119(6):873–887.
30. Bertholet AM, Millet AM, Guillermin O, et al. OPA1 loss of function affects in vitro neuronal maturation. *Brain* 2013; 136(Pt 5):1518–1533.
31. Savini G, Carbonelli M, Parisi V, Barboni P. Repeatability of optic nerve head parameters measured by spectral-domain OCT in healthy eyes. *Ophthalmic Surg Lasers Imaging* 2011; 42(3):209–215.
32. Ito Y, Nakamura M, Yamakoshi T, Lin J, Yatsuya H, Terasaki H. Reduction of inner retinal thickness in patients with autosomal dominant optic atrophy associated with OPA1 mutations. *Invest Ophthalmol Vis Sci* 2007;48(9):4079–4086.
33. Rönnbäck C, Milea D, Larsen M. Imaging of the macula indicates early completion of structural deficit in autosomal-dominant optic atrophy. *Ophthalmology* 2013;120(12): 2672–2677.
34. Barboni P, Valentino ML, La Morgia C, et al. Idebenone treatment in patients with OPA1-mutant dominant optic atrophy. *Brain* 2013;136(Pt 2):e231.
35. Schimpf S1, Fuhrmann N, Schaich S, Wissinger B. Comprehensive cDNA study and quantitative transcript analysis of mutant OPA1 transcripts containing premature termination codons. *Hum Mutat* 2008;29(1):106–112.
36. Marchbank NJ, Craig JE, Leek JP, et al. Deletion of the OPA1 gene in a dominant optic atrophy family: evidence that haploinsufficiency is the cause of disease. *J Med Genet* 2002; 39(8):e47.
37. Amati-Bonneau P, Valentino ML, Reynier P, et al. OPA1 mutations induce mitochondrial DNA instability and optic atrophy "plus" phenotypes. *Brain* 2008;131(Pt 2):338–351.
38. Yu-Wai-Man P, Griffiths PG, Gorman GS, et al. Multi-system neurological disease is common in patients with OPA1 mutations. *Brain* 2010;133(Pt 3):771–786.

Biosketch

Dr Piero Barboni graduated at Bologna's University (Italy) in 1986 and completed his medical and surgical ophthalmological training at Bologna's University in 1990. He has worked as neuro-ophthalmologist consultant at Scientific Institute San Raffaele, Milan, since 2012. He's devoted to the study of hereditary optic neuropathies, for which he has collaborated with several university-based centers (Bologna, Los Angeles, Tubingen, Sao Paulo). He has authored more than 80 papers on international peer-reviewed journals and several books.

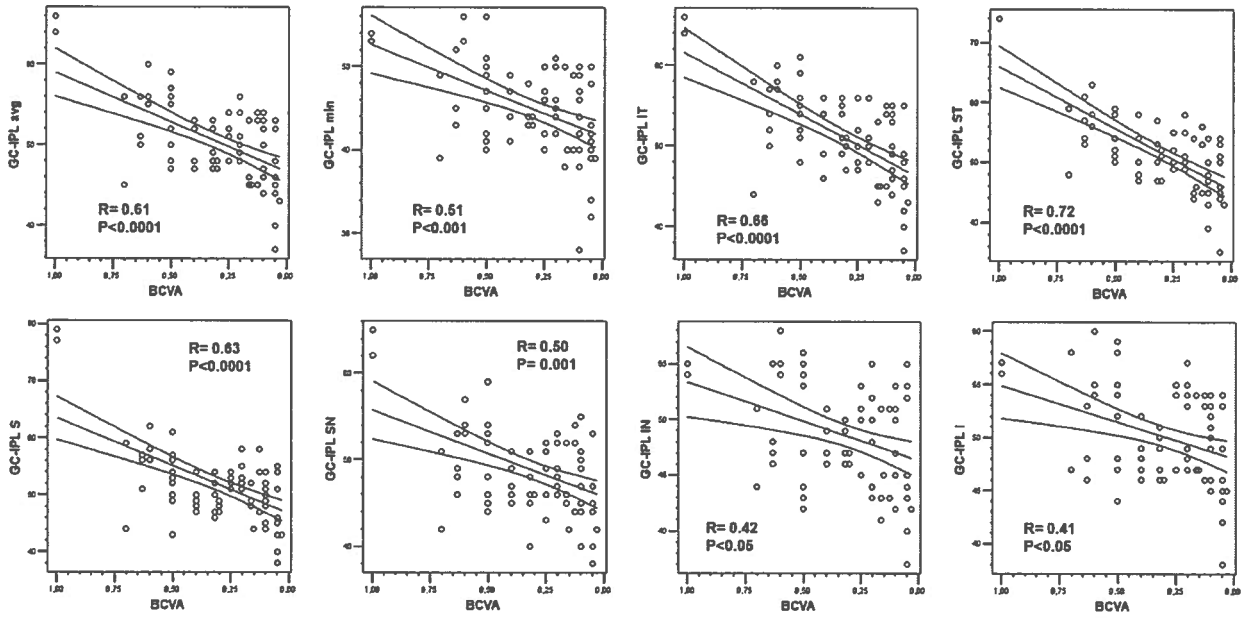

SUPPLEMENTAL FIGURE 1. Plot showing the correlation between Macular Ganglion Cell-Inner Plexiform Layer (GC-IPL) thickness, as average and minimum and at level of the different sectors, and best corrected visual acuity (BVCA) in patients with dominant optic atrophy. Regression lines and 95% confidence intervals are shown.

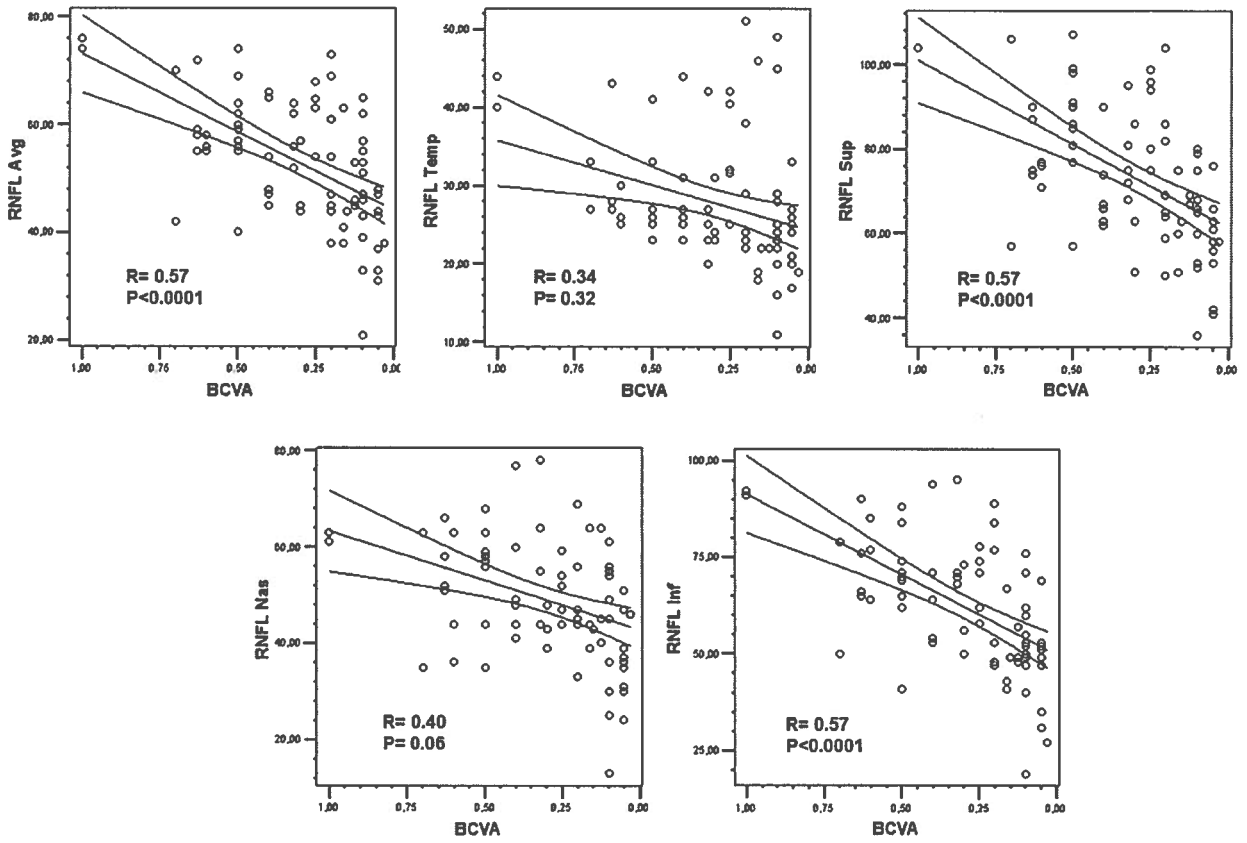

SUPPLEMENTAL FIGURE 2. Plot showing the correlation between Retinal Nerve Fiber Layer (RNFL) thickness, as average and at level of the different quadrants, and best corrected visual acuity (BVCA) in patients with dominant optic atrophy. Regression lines and 95% confidence intervals are shown.